ACS OMEGA

http://pubs.acs.org/journal/acsodf

Article

Kidney ECM Pregel Nanoarchitectonics for Microarrays to Accelerate Harvesting Gene-Edited Porcine Primary Monoclonal Spheres

Mengyu Gao,[⊥] Xinglong Zhu,[⊥] Wanliu Peng, Yuting He, Yi Li, Qiong Wu, Yanyan Zhou, Guangneng Liao, Guang Yang, Ji Bao,* and Hong Bu*

Cite This: *ACS Omega* 2022, 7, 23156−23169

Read Online

ACCESS | Metrics & More | Article Recommendations | Supporting Information

ABSTRACT: One of the key steps of using CRISPR/Cas9 to obtain gene-edited cells used in generating gene-edited animals combined with somatic cell nuclear transplantation (SCNT) is to harvest monoclonal cells with genetic modifications. However, primary cells used as nuclear donors always grow slowly and fragile after a series of gene-editing operations. The extracellular matrix (ECM) formulated directly from different organs comprises complex proteins and growth factors that can improve and regulate the cellular functions of primary cells. Herein, sodium lauryl ether sulfate (SLES) detergent was first used to perfuse porcine kidney ECM, and the biological properties of the kidney ECM were optimized. Then, we used a porcine kidney ECM pregel to pattern the microarray and developed a novel strategy to shorten the time of obtaining gene-edited monoclonal cell spheroids with low damage in batches. Our results showed that the SLES-perfused porcine kidney ECM pregel displayed superior biological activities in releasing growth factors and promoting cell proliferation. Finally, combined with microarray technology, we quickly obtained monoclonal cells in good condition, and the cells used as nuclear donors to construct recombinant embryos showed a significantly higher success rate than those of the traditional method. We further successfully produced genetically edited pigs.

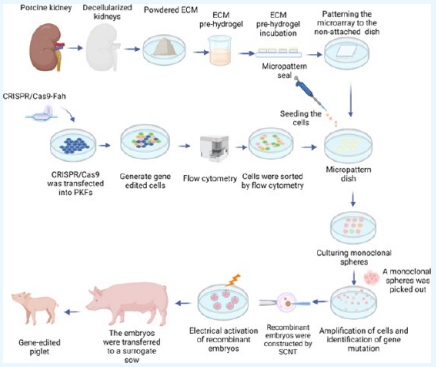

1. INTRODUCTION

Gene-edited pigs have been extensively used as research models for human disease pathogenesis, xenotransplantation, and gene therapy due to anatomical and physiological similarities to humans.[1]

Tyrosinemia type I (HT1) is an autosomal-recessive hereditary disease caused by the deletion of the fumarylacetoacetate hydrolase (*Fah*) gene. Deletion of the *Fah* gene leads to the accumulation of fumarylacetoacetate (FAA), a toxic metabolite, resulting in severe liver damage and most frequently leading to death if untreated. 2-(2-Nitro-4-trifluoromethylbenzoyl)-1,3 cyclohexanedione (NTBC) is a commonly used treatment.[2] We aimed to knock out the *Fah* gene in Bama miniature pigs and provide a large animal model for the pathogenesis of HT1 disease and gene therapy. In addition, Fah/Rag2/Il2rg knockout mice have been used to produce bioengineered mice with humanized liver cells.[3] The liver injury gene knockout pig model can also provide an ecological niche for heterogeneous liver cell proliferation, and the gene-editing pig can be used as a bioreactor to amplify human liver cells.

At present, clustered regularly interspaced short palindromic repeat (CRISPR)/CRISPR-associated 9 (CRISPR/Cas9) technology has been widely used to generate gene-editing animal models.[4] Edited somatic cells with CRISPR/Cas9 followed by somatic cell nuclear transfer (SCNT) are one of the most common methods to produce gene-edited pigs.[5] The process of SCNT involves editing somatic cells using CRISPR/Cas9 and picking out the gene-editing monoclonal cells and then using the edited somatic cells as nuclear donors to construct recombinant embryos, which are then activated by electricity and transplanted into surrogate sows to produce gene-edited pigs. The advantage of SCNT is that researchers can precisely screen cells with specific mutations in vitro and then use those cells as nuclear donors to create a series of known and characterized offspring.[6] In the process of SCNT, obtaining gene-edited nuclear donor cells in good condition is an important step in the preparation of gene-edited pigs. The quality of the cells will directly affect the development of recombinant embryos in the later stage, so it is the key and prerequisite for the production of gene-edited pigs.[7]

Currently, the nuclear donor cells used for SCNT are mainly porcine embryonic fibroblasts or porcine renal fibroblasts (PKFSs).[8] After gene editing of somatic cells in vitro, it is necessary to select and amplify the positive gene-editing monoclonal cells, which can be used as nuclear donors to

Received: February 22, 2022
Accepted: May 19, 2022
Published: June 29, 2022

transplant into mature oocytes without nucleation. At present, the commonly used methods to obtain gene-edited monoclonal cells are the limit dilution method or clone cycle digestion method. Single cells were sorted into Petri dishes by limiting dilution or flow cytometry. Due to the lack of a microenvironment for cell population growth, single cells proliferated slowly, and some cells could not proliferate normally in a single-cell environment. However, harvesting monoclonal cells with clone rings still faces a long monoclonal growth cycle, and mechanical force damage during harvesting monoclonal cells will significantly reduce cell activity and nuclear reprogramming ability, affecting the development of recombinant embryos.[9,10] Therefore, harvesting monoclonal cells using the above two traditional methods is faced with the problems of a long cycle and low efficiency and is a rate-limiting step in the production of gene-edited pigs.[11]

The patterned microarray was applied to the growth of cell spheres, in which cells could be restrictively adhered to the microarray and spontaneously assemble into spheroids.[12] Our preliminary study also showed that a conventional fibronectin-derived microarray could be used to culture monoclonal cells of cell lines, but after preliminary experiments, the microarray could not support the primary cells to gather into a spheroid, which could be used as a nuclear donor.

Fibronectin, collagen I, collagen IV, and Matrigel as substrates are mainly used for traditional microarrays.[13] However, a single protein component is not enough to improve and regulate the viability and functions of specific cells or primary cells.[14]

In some recent studies, the extracellular matrix (ECM) derived from a variety of soft tissues, such as the small intestine, bladder, kidney, liver, and lung,[15−17] can provide an ideal microenvironment for cells, with tissue specificity to mediate cell adhesion, proliferation, differentiation, gene expression, migration, and assembly.[18] Due to its superior biosecurity and inherent regulation and support for seeded cells, ECM pregel would be an ideal substrate for microarrays to support the proliferation and growth of gene-edited primary cells.[19]

The ideal detergent should be able to fully remove cells while retaining the ECM protein to the maximum extent. Sodium dodecyl sulfate (SDS) is an ionic detergent with a hydrophilic negative charge on the head that can dissolve the cytoplasm, cell nucleus, and cell membrane, and it is the most commonly used detergent in tissue engineering. However, SDS causes collagen depletion and can damage tissue ultrastructure and lead to excessive loss of extracellular matrix components such as key growth factors.[20] Sodium lauryl ether sulfate (SLES) is a novel anionic detergent. Recent studies reported that SLES has been used to prepare the extracellular matrix of rat heart,[21] liver,[22] kidney,[23] lung,[24] and porcine lung extracellular matrix,[17] and SLES showed milder chemical properties and higher biocompatibility than SDS. In addition, SLES showed better preservation of proteoglycans, cytokines (such as basic FGF), and ECM microstructures than SDS, which indicated that SLES-treated decellularized scaffolds could be superior to those treated with SDS as substrates for cell growth.[25] One of the reasons could be that SLES contains an ethoxyl group, which makes the chemical properties milder than those of SDS.

In this study, we attempted to use the novel anionic detergent, SLES, to decellularize the porcine kidney to obtain a kidney ECM pregel and firstly use it to pattern microarrays. This is the first time that such ECM-based microarrays are used to rapidly obtain gene-edited monoclonal primary cell spheres. The success rate of constructing recombinant embryos from monoclonal cells obtained by this method was significantly higher than that of the traditional cloning ring method. It could shorten the amplification cycle of monoclonal cells in vitro, maintain a good cell state, and provide high-quality nuclear donors for somatic cell nuclear transplantation.

2. MATERIALS AND METHODS

2.1. Animals. The kidneys were harvested from 12 to 15 kg Bama miniature pigs (Guangxi, China) for use as ECM donors. Porcine kidney fibroblasts (PKFs) were isolated from newborn Bama miniature pigs. All animal care and experiments complied with the guidelines of the Animal Experiment Center of Sichuan University, and this study was approved by the Ethics Committee of Sichuan University for Animal Research.

2.2. Decellularization of Porcine Kidney. Animals were anesthetized with Zoletil 50 (10 mg kg^{-1} body weight, Virbac, France) by intramuscular injection and maintained with propofol (6 mg kg^{-1} h^{-1}, Qingyuan Jiabo, China) through ear vein injection. The renal aorta of the kidney was cannulated and perfused twice with phosphate-buffered saline (PBS) to remove the blood and then frozen at −20 °C for at least 24 h. Once the organs were thawed at room temperature, distilled water was perfused at a flow rate of 15 mL min^{-1} for 3 h. To compare two different detergents of decellularization, in the first group, 1% Triton (Sigma-Aldrich, #X100), 1% sodium dodecyl sulfate (SDS, Sigma-Aldrich, #L3771), and 1% Triton (Sigma-Aldrich, #X100) were perfused into the kidney at a flow rate of 15 mL min^{-1} for 3 h, 16 h, and 3 h, respectively. In the second group, 1% Triton, 1% SLES, and 1% Triton were perfused at the same rate. Finally, to remove the residual detergents, distilled water was perfused into the scaffolds for 1 h. The decellularized kidneys were stored at −80 °C or fixed with 4% formalin or 2.5% glutaraldehyde until use.

2.3. Assessment of ECM. *2.3.1. Histological Analysis of ECM.* The native and decellularized tissue samples were fixed in 4% paraformaldehyde and embedded in paraffin. The paraffin sections (4 μm thick) were stained with hematoxylin and eosin (H&E) to visualize the nuclei and tissues. Nuclear-specific 4,6-diamidino-2-phenylindole (DAPI) staining was performed to detect the efficacy of cell removal. We further examined the morphology of the ECM by scanning electron microscopy (SEM). The native and decellularized tissues were fixed in 2.5% glutaraldehyde (Sigma-Aldrich, #G5882) for at least 24 h. Samples were then washed with distilled water and dehydrated in a graded ethanol series. Dehydrated samples were subsequently dried at the critical point (HCP2; Hitachi, Tokyo, Japan) and sputter-coated with gold−palladium. Electron micrographs of kidney ECM were obtained at 5.0 kV and 500× magnification by a Hitachi S-4800 SEM (Hitachi, Japan).

To evaluate the retention of the crucial proteins in the ECM, sections of native and decellularized tissues were subjected to Masson's trichrome and immunofluorescence (IF) staining according to established protocols. The collagen content was quantified using a colorimetric assay to detect hydroxyproline.[26] Primary antibodies against collagen I (ab6308, 1:500, Abcam, Massachusetts), collagen IV (ab6586, 1:500, Abcam), fibronectin (ab6328, 1:200, Abcam), and laminin (ab11575, 1:200, Abcam) were used. For immunofluorescence, the sections were incubated with secondary antibodies and DAPI at room temperature in the dark for 1 h and 5 min, respectively. The images were captured using an N-SIM-S super resolution microscope (Nikon, Japan).

https://doi.org/10.1021/acsomega.2c01074
ACS Omega 2022, 7, 23156−23169

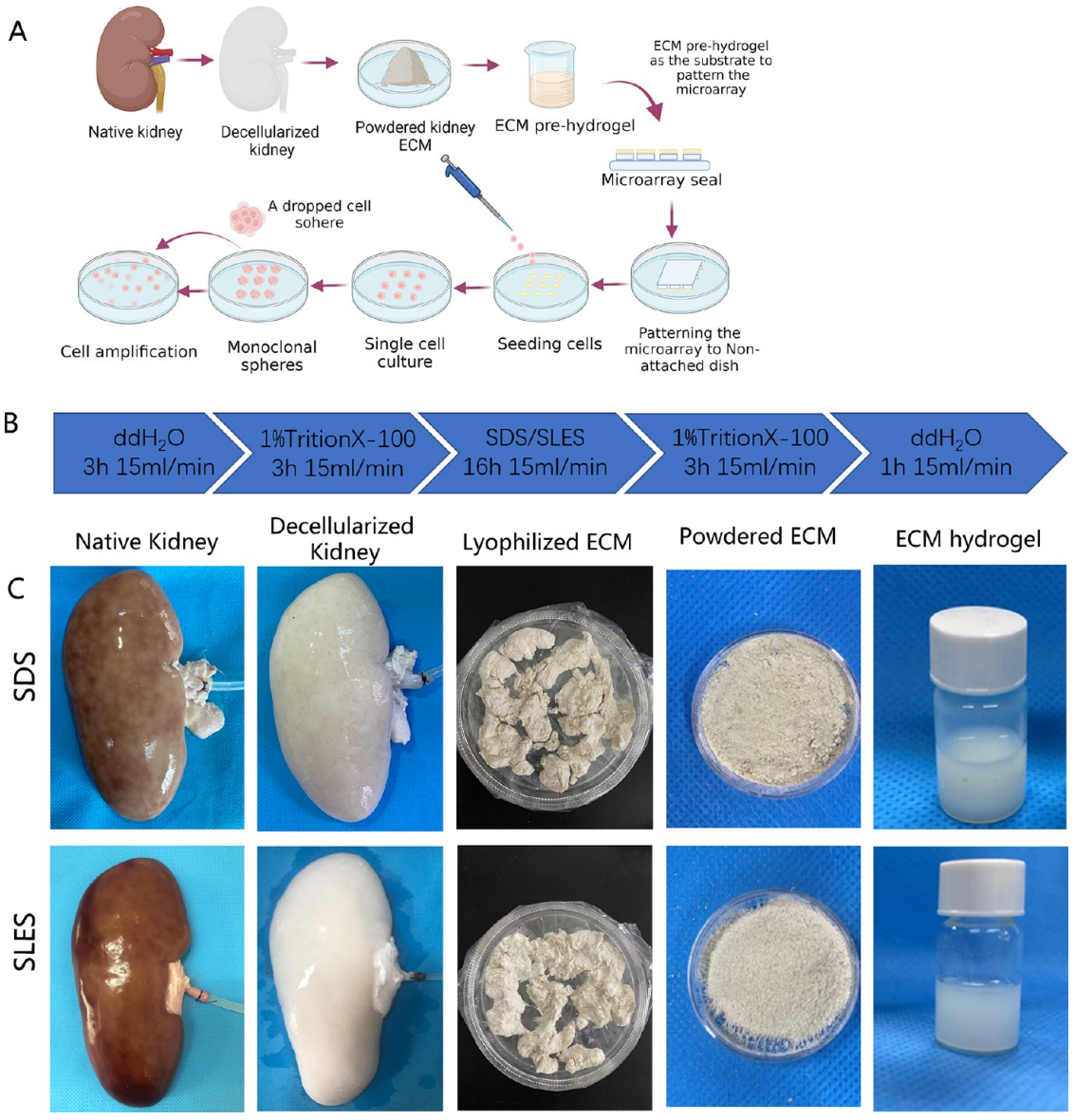

Figure 1. Process of generation of monoclonal cells using microarrays and preparation of porcine kidney ECM and kidney ECM pregel. (A) The porcine kidney ECM was lyophilized, powdered, and digested to prepare the ECM pregel, and then the ECM pregel was used to pattern the microarray. The gene-edited cells were seeded into the microarray and proliferated to become monoclonal cell spheres. ECM: extracellular matrix. (B) Perfusion process of porcine kidney ECM. (C) SDS/SLES kidney ECM was lyophilized, powdered, and digested to prepare the ECM pregel.

2.3.2. DNA Content Quantification. To evaluate the effectiveness of DNA removal. The DNA of native and decellularized tissues was isolated from samples with a TissueNeasy Kit (Tiangen Biotech Corporation, Beijing, China) and detected by a NanoDrop spectrophotometer (ND-2000c, Thermo).

2.3.3. Component Analysis of ECM. Fourier transform infrared spectrometry (FTIR, Nicolet 560) was used to detect the functional groups of the ECM.

Collagen content in the tissues was quantified by a colorimetric assay to detect hydroxyproline, as described previously. The freeze-dried natural kidney tissue and the decellularized kidney tissue were weighed to the same weight and hydrolyzed overnight with papain at a concentration of 140 μg mL^{-1} at 60 °C. After hydrolysis, neutralization, and oxidation, p-dimethylaminobenzaldehyde was added, and the samples were quantified by measuring the absorbance at 570 nm.

The glycosaminoglycan (GAG) content of the ECM was quantified using the Blyscan GAG assay kit (Biocolor, U.K.). The samples were quantified by measuring the absorbance at 650 nm.

The content of growth factors (bFGF, VEGF) in ECM was detected by ELISA (RuiXin, RX500921P, China; RuiXin, RX500812P, China).

To detect the protein composition of the SDS-treated ECM and SLES-treated ECM, proteomics was performed by liquid chromatography-tandem mass spectrometry (LC−MS/MS) analysis. The raw MS data for each sample were analyzed using the "Wu Kong" platform (https://www.omicsolution.com/wkomics/main/).

2.4. Preparation of ECM Pregel from Kidney ECM. The ECM was lyophilized using a lyophilizer (EYELA, FDU-2110, Japan) and powdered with a Wiley Mill (Retsch, MM400, Germany). Then, they were dissolved in 10% (w/w) pepsin

https://doi.org/10.1021/acsomega.2c01074
ACS Omega 2022, 7, 23156−23169

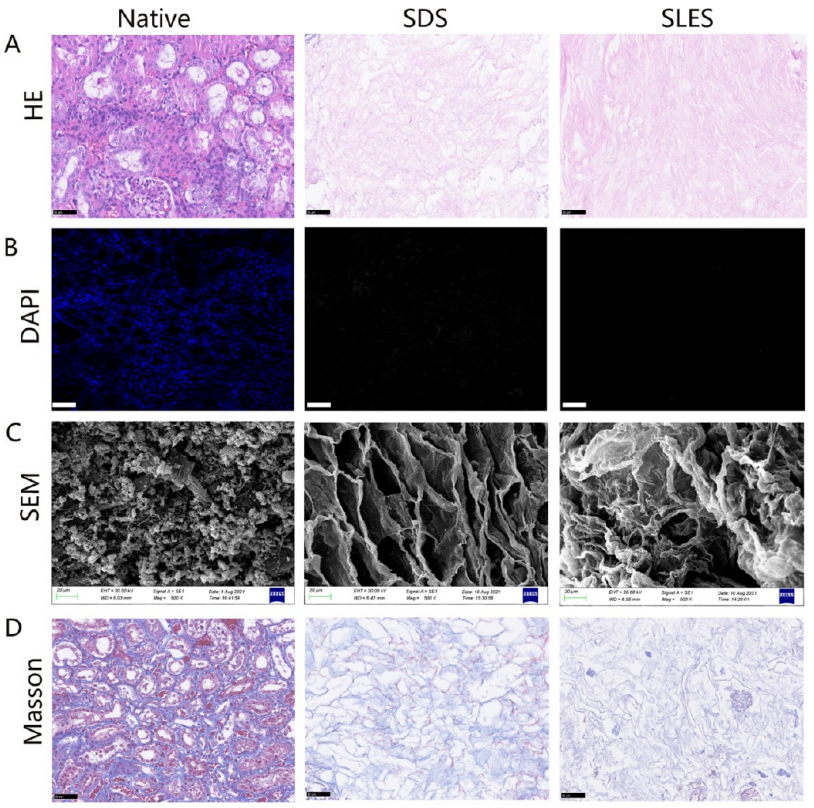

Figure 2. Characteristics of porcine kidney ECM. (A) Hematoxylin and eosin (H&E) staining of native kidney and ECM. Scale bar = 50 μm. (B) 4,6-Diamidino-2-phenylindole (DAPI) staining (scale bar = 100 μm); (C) Scanning electron microscopy (SEM) images of native kidney and ECMs (scale bar = 20 μm); (D) Masson's trichrome staining of native kidney and ECM scaffolds. Collagen is blue−purple, the cytoplasm is pink, and the nucleus is dark blue or black. Scale bar = 50 μm.

(Sigma-Aldrich) in 0.01 M HCl with constant stirring for 48 h at room temperature. Subsequently, the pH of the ECM solution was adjusted to 7.2−7.4 using 0.1 M NaOH.[27] The final pregel solution was induced to form a hydrogel after incubation for 30 min at 37 °C.

2.5. Biological Evaluation of ECM Pregel. The biological evaluation of ECM pregel as a substrate was performed using primary porcine kidney fibroblasts (PKFs). PKFs were isolated from newborn Bama piglets, as previously described.[8] They were maintained in DMEM (Gibco, China) with 10% fetal bovine serum (FBS) (Gibco, Australia) and 1% penicillin−streptomycin solution (HyClone, China) in a 5% CO_2 incubator at 37 °C.

To determine whether the kidney ECM hydrogels could support cell viability, adhesion, and proliferation, the kidney ECM solution (10 mg mL^{-1}) was diluted with PBS to a final concentration of 0.2 mg mL^{-1} and coated on 24-well plates and 96-well plates. The same concentration of Matrigel solution-treated plates was used as a comparison group, and uncoated plates were used as controls. The coated plates were incubated at 37 °C for 1 h and then washed three times with PBS. Then, the plates were exposed to UV light (365 nm) for 1 h. The coated plates were stored at 4 °C.

The cell adhesion percentage after 4 h of cell seeding was evaluated by counting the nonadhered cells using Countess TM II FL (Invitrogen). PKFs were seeded on the plates, and cell viability was examined by FluoroQuench fluorescent stain (One Lambda; Thermo Fisher Scientific, Inc., Waltham, MA) after 1, 3, and 5 days in culture. The images were analyzed using a fluorescence microscope (OBSERVER D1/AX10 cam HRC, Carl Zeiss, Oberkochen, Germany). Cell Counting Kit-8 (CCK-8, Sigma-Aldrich) and EdU (RIBOBio, C10310-1, China) assays were used to evaluate cell proliferation. The concentration of growth factor in the cell culture supernatant was detected by ELISA (RuiXin, RX500921P, China; RuiXin, RX500812P, China).

2.6. Microarray Patterning. A poly (dimethylsiloxane) (PDMS) seal was obtained by means of a laser etching characteristic pattern on a silicon wafer. To screen for a size suitable for PKFs to grow into spheres, microarrays with diameters of 50, 100, 200, and 50 μm spacing between microarrays were used as templates. Then, the cells were incubated with 0.2 mg mL^{-1} kidney ECM substrates mixed with 2 μg fluorescein isothiocyanate isomer for 20 min at room temperature, and the substrates on the microarray surfaces were subsequently removed. The microarray was dried at 37 °C for 10 min.

The seals were patterned into 35 mm diameter nontreated cell culture dishes at 0.2 N force for 10 min. The shapes of the microarray were observed by fluorescence microscopy (OBSERVER D1/AX10 cam HRC, CARL ZEISS, Germany). Subsequently, the treated dishes were coated with 10 g L^{-1} pluronic F-127 water solution (Sigma-Aldrich) for 1 h to prevent nonspecific cellular adherence and then sterilized through ultraviolet irradiation for 1 h.

2.7. Generation of *Fah* Gene Knockout Cells. The sgRNA targeting *Fah* was used in our previous research (5′-GCGATTGGTGACCAGATCC-3′). Then, the oligonucleotides of sgRNA were ligated to the PX458 vectors. Targeting plasmids for the *Fah* genes were cotransfected into PKF cells with Lipofectamine 3000 (Lipofectamine TM3000, Invitrogen).

https://doi.org/10.1021/acsomega.2c01074
ACS Omega 2022, 7, 23156−23169

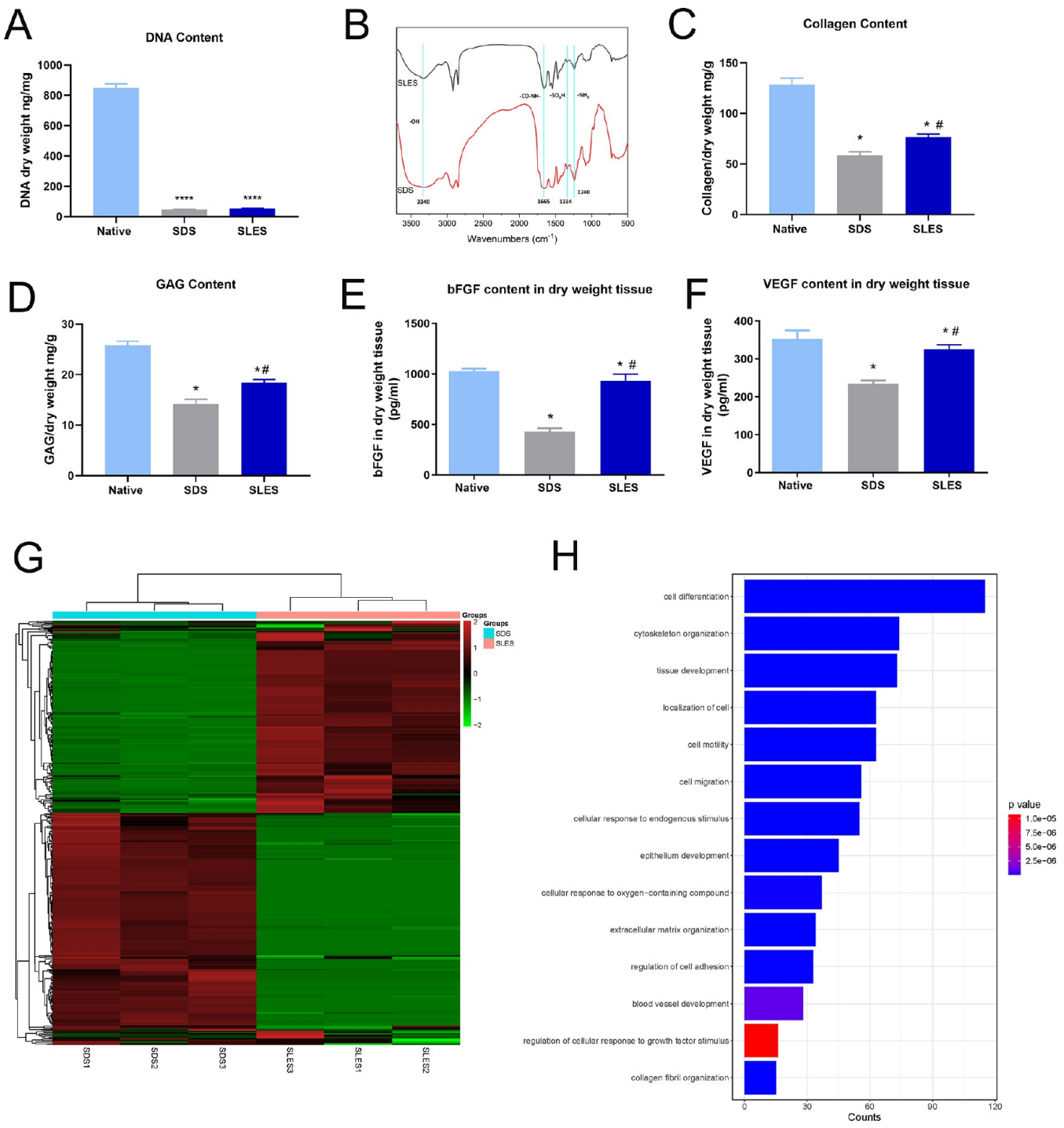

Figure 3. Detection of the kidney ECM content. (A) Quantification of the DNA content in native kidney and ECM scaffolds ($n = 3$, $^{*}p < 0.05$ versus the native group). (B) FTIR spectra of SDS-treated and SLES-treated ECMs. Evaluation of the collagen content (C), GAG content (D), growth factors of bFGF (E) and VEGF (F) in native and decellularized kidneys ($n = 3$). $^{*}p < 0.05$ versus the native group; $^{\#}p < 0.05$ versus the SDS group. G: Protein clustering analysis of SDS-treated and SLES-treated ECMs. H: KEGG signal pathway analysis for the differentially expressed proteins in SDS-treated and SLES-treated ECMs.

After 48 h of transfection, the GFP-positive cells were sorted by flow cytometry (FACSAria SORP, BD). To detect the modifications, genomic DNA was extracted from cells and subjected to polymerase chain reaction (PCR) with TaKaRaTaq Hot Start Version (TaKaRa, Japan) and Sanger sequencing using specific primers (Fw: 5′-GCTGTGAGCTGTGGTGTA-CATTG-3′; Rv: 5′- GTAGCTCCGATTCACCTGCTAG-3′).

2.8. Harvesting the Gene-Edited Monoclonal Cells by Microarray. The PKFs sorted by flow cytometry were plated on a microarray with diameters of 50 μm (planted with 1×10^3 cells). A single cell is confined to a point of the microarray and grows into a sphere. The process of generating monoclonal cells using microarrays is shown in Figure 1A. The morphology of cellular spheres was observed by EVOS TM XL Core (Invitrogen) at four consecutive days in culture. Cell spheres

https://doi.org/10.1021/acsomega.2c01074
ACS Omega 2022, 7, 23156−23169

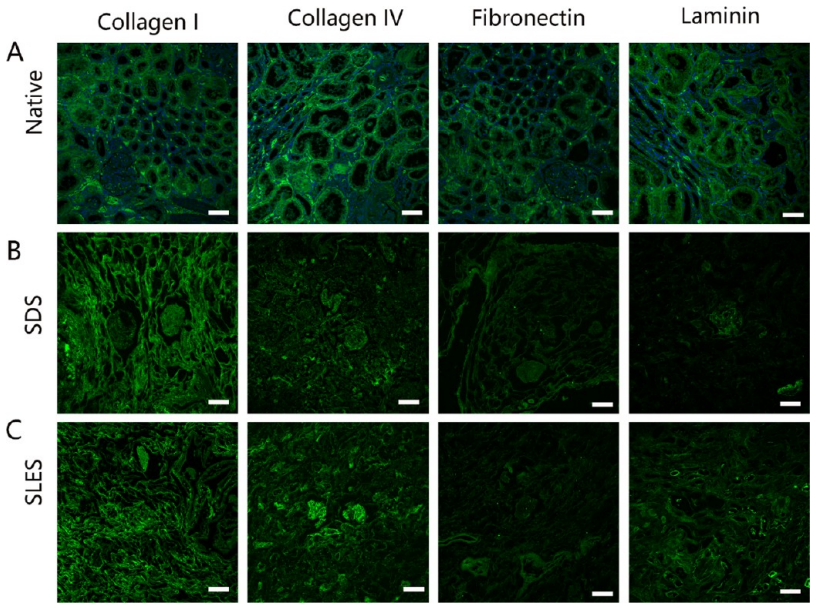

Figure 4. Immunofluorescence staining for ECM protein components. Collagen I, collagen IV, fibronectin, and laminin immunofluorescence staining of native (A) kidneys, SDS-treated ECM (B), and SLES-treated ECM (C). Scale bar = 100 μm.

derived from single cells were removed with a pipette gun. After 3−5 days of amplification culture, 1/10 of the cells were used for genotyping, and the rest were cryopreserved for SCNT. Then, immunofluorescence (IF) of the gene-edited cells was performed with primary antibodies against Fah (bs-16194R; Bioss, China). The IF slides of the cells were analyzed by a fluorescence microscope (AX10 imager A2/AX10 cam HRC; Zeiss). At the same time, monoclonal cells were obtained by the traditional cloning ring method as a comparison group to compare the proliferation time and growth state of cells. The sorted cells were seeded in a 6 cm Petri dish, and the monoclonal cells were selected by a glass cloning ring combined with trypsin digestion.

2.9. Generation of Gene-Edited Porcine Embryos and Pigs by SCNT. After identifying the positive clones, SCNT was conducted, as described previously.[6] First, fresh ovaries are collected from the slaughterhouse, and oocytes are harvested and cultured in vitro until the second meiosis (MII). Subsequently, the gene-edited somatic cells were used as nuclear donors and injected into the enucleated oocytes under the embryo microinjection apparatus, and the recombinant embryos were electrically fused/activated using the cell fusion apparatus.

To produce gene-edited pigs, one surrogate sow received 250 embryos. The sow was fed NTBC daily. Abdominal ultrasound was performed 1 month after SCNT to determine pregnancy. Approximately 114 days later, piglets were delivered by natural birth.

For analysis of *Fah* genotypes in the obtained piglets, the genomic DNA of ear tissues was extracted. PCR and Sanger sequencing were performed as described above. The liver morphology of *Fah*KO pigs was observed by H&E staining.

2.10. Statistical Analysis. All data were analyzed using SPSS statistical software (version 17.0) and organized using GraphPad Prism software (La Jolla, CA). Dunnett's *t*-test was used to compare data sets between two groups. $P < 0.05$ was accepted as significant.

3. RESULTS

3.1. Kidney Decellularization and ECM Content Detection. As shown in Figure 1B, kidney ECM was obtained by two reagents, and the kidney ECM was powdered and digested to prepare the ECM pregel. Visual inspection showed that SDS-treated kidneys were more transparent than SLES-treated kidneys (Figure 1B).

In comparison with the native kidney, both the 1% SDS and 1% SLES decellularized solutions almost completely removed the nuclear material, as shown by H&E or DAPI staining and DNA quantification (Figures 2A,B and 3A). H&E and DAPI staining confirmed that visible cell components were removed by SDS and SLES. Remarkable differences in the ultrastructure were observed via SEM in native and ECMs (Figure 2C). Furthermore, the SLES-treated ECM exhibited a denser structure than SDS-treated ECM, which indicated that SLES may be a milder detergent with better preservation of ultrastructure integrity than SDS. Masson's trichrome staining showed that the protein composition was well preserved (Figure 2D).

For the chemical structure analysis, FTIR results showed that both the SLES-treated ECM pregel and SDS-treated ECM pregel contained hydroxyl groups, amide groups, sulfonic groups, and amino functional groups (Figure 3B). The amide group was assigned to the presence of collagen, while the hydroxyl group signal was used to indicate proteoglycans.[28] Collagen and glycosaminoglycan (GAG) are the main components of the ECM, so we then detected the content of collagen and GAG. The results showed that collagen retention and GAG retention in the SLES groups were significantly higher than those in the SDS group (Figure 3C,D).

The ELISA results (growth factors of bFGF and VEGF) indicated that both SDS-treated and SLES-treated ECM could effectively retain cytokines (Figure 3E,F). The SLES-treated ECM retained a higher level of growth factors than the SDS-treated ECM ($^*p < 0.05$).

To show the components of ECMs more directly and compare the differences between the SLES-treated ECM and

https://doi.org/10.1021/acsomega.2c01074
ACS Omega 2022, 7, 23156−23169

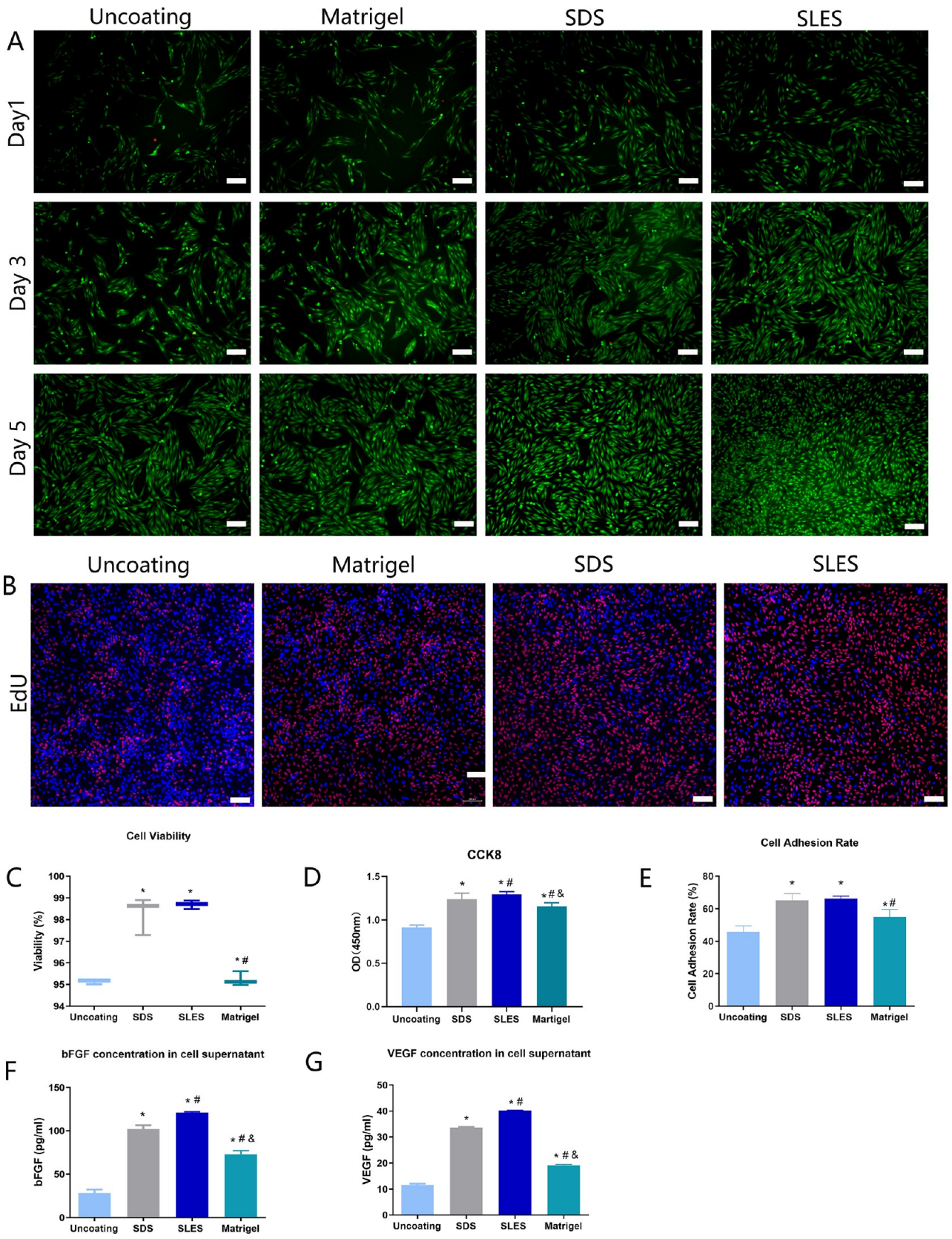

Figure 5. Biological evaluation of kidney ECM-coated plates. (A) Live/dead images of PKFs (green-live, red-dead). Scale bar = 100 μm. (B) Cell proliferation of PKFs after 24 h of culture in coated plates by EdU detection. Scale bar = 100 μm. (C) The viability of PKFs cultured on each substrate ($n = 3$). (D) Proliferation of PKFs (cck-8) on day 1 after cell seeding ($n = 3$). (E) The percentage of PKF adhesion 4 h after cell seeding ($n = 3$). (F, G) bFGF and VEGF concentrations in the cell culture supernatant at 24 h after cell seeding ($n = 3$). $^{*}p < 0.05$ versus the native group; $^{\#}p < 0.05$ versus the SDS group. $^{\&}p < 0.05$ versus the Matrigel group.

https://doi.org/10.1021/acsomega.2c01074
ACS Omega 2022, 7, 23156−23169

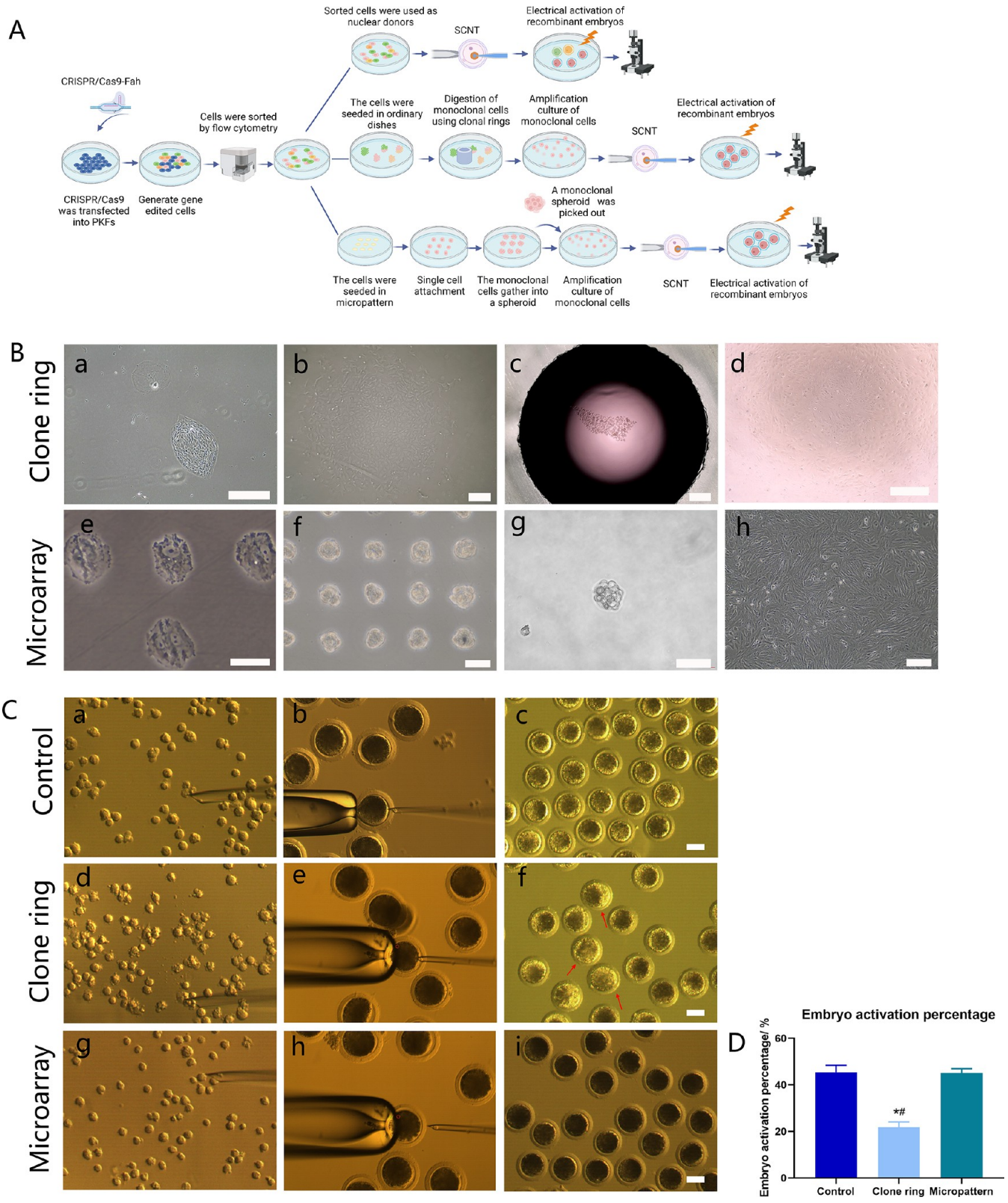

Figure 6. Evaluation of the effect of producing recombinant embryos from monoclones obtained by microarrays. (A) The flow chart for the comparison study. Flow cytometry only enriched the cells positively transfected with the PX458 plasmid. There were still gene-edited cells and unedited cells, which required monoclonal selection and sequencing verification. Green represents cells that were only transfected with the PX458 plasmid but did not undergo gene editing; red represents cells with homozygous mutations; yellow represents cells with heterozygous mutations. The cells not subjected to monoclonal screening were used as controls to construct recombinant embryos. (B) Monoclonal cells were obtained by cloning rings and microarrays. (a) The cells sorted by flow cytometry were cultured in a 6 cm dish, and monoclonal cell populations were observed on day 7; scale bar = 100 μm. (b) The monoclonal clones were morphologically changed during proliferation; scale bar = 100 μm. (c) Digestion of monoclonal cell populations using glass cloning rings; scale bar = 200 μm. (d) The morphology of monoclonal cells changed during the proliferation process in 24-

https://doi.org/10.1021/acsomega.2c01074
ACS Omega 2022, 7, 23156−23169

Figure 6. continued

well plates; scale bar = 100 μm. (e and f) The cells were attached to the microarray after 12 h and 96 h. (g) A harvested monoclonal sphere from the microarray at 5 days. (h) Monoclonal cells were amplified and cultured for 72 h. Scale bar of e−h = 50 μm. (C) Construction and electrical activation of recombinant embryos. The somatic nuclear donors, injected nuclear donors into mature oocytes, and electrically activated embryos are shown from left to right. Scale bar = 100 μm. (D) Embryo activation efficiency (n = 3). *p < 0.05 versus the control group; #p < 0.05 versus the micropattern group.

SDS-treated ECM, we performed cluster analysis on the proteins identified by proteomics (Figure 3G), which showed that there was some homology and difference in protein composition between the two groups. Furthermore, the differential proteins were analyzed for KEGG functional pathway enrichment, and the results showed that the differential proteins between the two groups were concentrated in cell differentiation, cytoskeleton organization, cell migration, regulation of cell adhesion, regulation of cellular response to growth factor stimulus, and so on (Figure 3H).

To further focus on the bioactive ingredients in the ECMs, immunofluorescence staining was performed on collagen I, collagen IV, fibronectin, and laminin. The results showed that all of them were well preserved (Figure 4).

3.2. In Vitro Biological Evaluation of Kidney ECM Pregel. For biological evaluation, PKFs were cultured on SDL-, SLES-, and Matrigel-coated plates and analyzed at 1, 3, and 5 days by live/dead images to indicate cell viability (Figure 5A,C). In the ECM-treated group, the survival rate was close to 100% (Figure 5C). The EdU and CCK-8 results showed that the proliferation of PKFs cultured on ECM-coated plates was significantly higher than that of PKFs cultured on Matrigel-coated and uncoated plates (Figure 5B,D). The ECM-coated group also had a higher number of adhered cells after 4 h of seeding than the other groups (Figure 5E). All of the results indicated that kidney ECM pregel could provide an adequate substrate for cell adhesion and proliferation and maintain a higher viability rate. The levels of bFGF and VEGF in the cell culture supernatant also showed a higher concentration in the ECM-coated group than in the Matrigel and uncoated groups (Figure 5F,G). Meanwhile, growth factor concentrations in the SLES group were significantly higher than those in the SDS group (Figure 5F,G, $^{\#}P < 0.05$). Based on the above results, we chose an SLES-treated ECM pregel as a substrate to prepare the microarray.

3.3. Rapid Generation of Gene-Edited Monoclonal Cells Using an ECM-Based Microarray and Evaluation of the Efficiency of Producing Recombinant Embryos. We explore whether using the microarray to obtain gene-edited monoclonal cells can shorten the harvest time of monoclonal cells and detect the effect of obtained monoclonal cells as nuclear donors for somatic cell nuclear transplantation. We chose the *Fah* gene to test the monoclonal harvesting platform. We packaged the high-efficiency sgRNA targeting *Fah*, which was verified in our previous study, into PX458 plasmid vectors.[29] The vectors were transfected into porcine kidney fibroblasts. Since PX458 carries green fluorescent protein (GPF), we sorted the GFP-positive cells by flow cytometry; that is, we enriched the gene-editing-positive cells as much as possible to obtain the gene-editing cell population.

We evaluated the effectiveness of using the microarray to obtain gene-edited monoclonal cells by comparing the efficiency of recombinant embryos. The sorted cells were divided into three groups. The flow diagram is shown in Figure 6A. In the first group, the sorted cells that did not undergo monoclonal selection and amplification were directly used as nuclear donors to construct recombinant embryos. After the reconstituted embryos were electrically activated, they were observed under a microscope. This group served as the control group.

In the second group, the sorted cells were plated into 6 cm dishes, and the growth of monoclonal cells was observed continuously. After the clone population grew to a certain size, the monoclonal cells were selected by a glass cloning ring combined with trypsin digestion. Monoclonal cells were used as nuclear donors to construct recombinant embryos. The electrically activated embryos were also viewed under a microscope. As shown in Figure 6B (cloning ring group), the cells proliferating from a single cell could be observed on days 7−10 (Figure 6B-a). Cell growth was relatively slow, and many monoclones changed their morphology due to long-term clonal proliferation instead of showing a regular fibrous shape (Figure 6B-b). Subsequently, the cells were digested by the clone ring (Figure 6B-c) and then cultured by continuous amplification on 96-well plates to 24-well plates (Figure 6B-d). It took nearly a month to obtain enough cells to serve as nuclear donors and freeze them. The morphology of most cultured cells changed.

In the third group, monoclonal cells were harvested using microarrays and used as nuclear donors to construct recombinant embryos and observe the state of electrically activated embryos under a microscope. To make a microarray suitable for the growth of PKF monoclonal cells, we first sequenced microarrays with diameters of 50, 100, and 200 μm to choose a suitable size for PKF growth into cell spheres (Figure S1). The cells could grow from an adherent state to a cell sphere both on the microarray with diameters of 50 and 100 μm (Figure S1A,B). However, in the microarray with a diameter of 200 μm, the cells did not demonstrate sphere formation trends (Figure S1C). As the 50 μm seal is more suitable for single-cell landing and the cell sphere viability of 50 μm was higher than that of 100 μm, the 50 μm diameter seal was selected for PKF monoclonal culture.

Figure 6B-e shows that one cell could grow at one position by controlling the cell density. After 24−48 h, the cells, planted in the microarray, began to grow from an adherent state to a three-dimensional (3D) structure and gradually formed a cell sphere. After 96 h, the cell spheres hardly continued to grow and remained at 50 μm (Figure 6B-f). On the 5th day, the cell spheres fell off after shaking or gently blowing with a pipette. After the spheres proliferating from a single cell were removed and blown (Figure 6B-g), the cells in good growth condition could be obtained quickly for 3−5 days by amplification culture (Figure 6B-h).

As shown in Figure 6C-a, after digestion, the cells without monoclonal screening had regular cell margins, and the recombinant embryos were constructed with compact and uniform cytoplasm after electrical activation (Figure 6C-c). However, most of the cells harvested using clone rings had irregular edges, such as “tentacles” (Figure 6C-d). Most of the recombinant embryos constructed by these cells as nuclear donors had loose cytoplasm and unclear cell membranes after electrofusion (Figure 6C-f). As unqualified embryos cannot develop properly, they will not be transferred to surrogate sows.

https://doi.org/10.1021/acsomega.2c01074
ACS Omega 2022, 7, 23156−23169

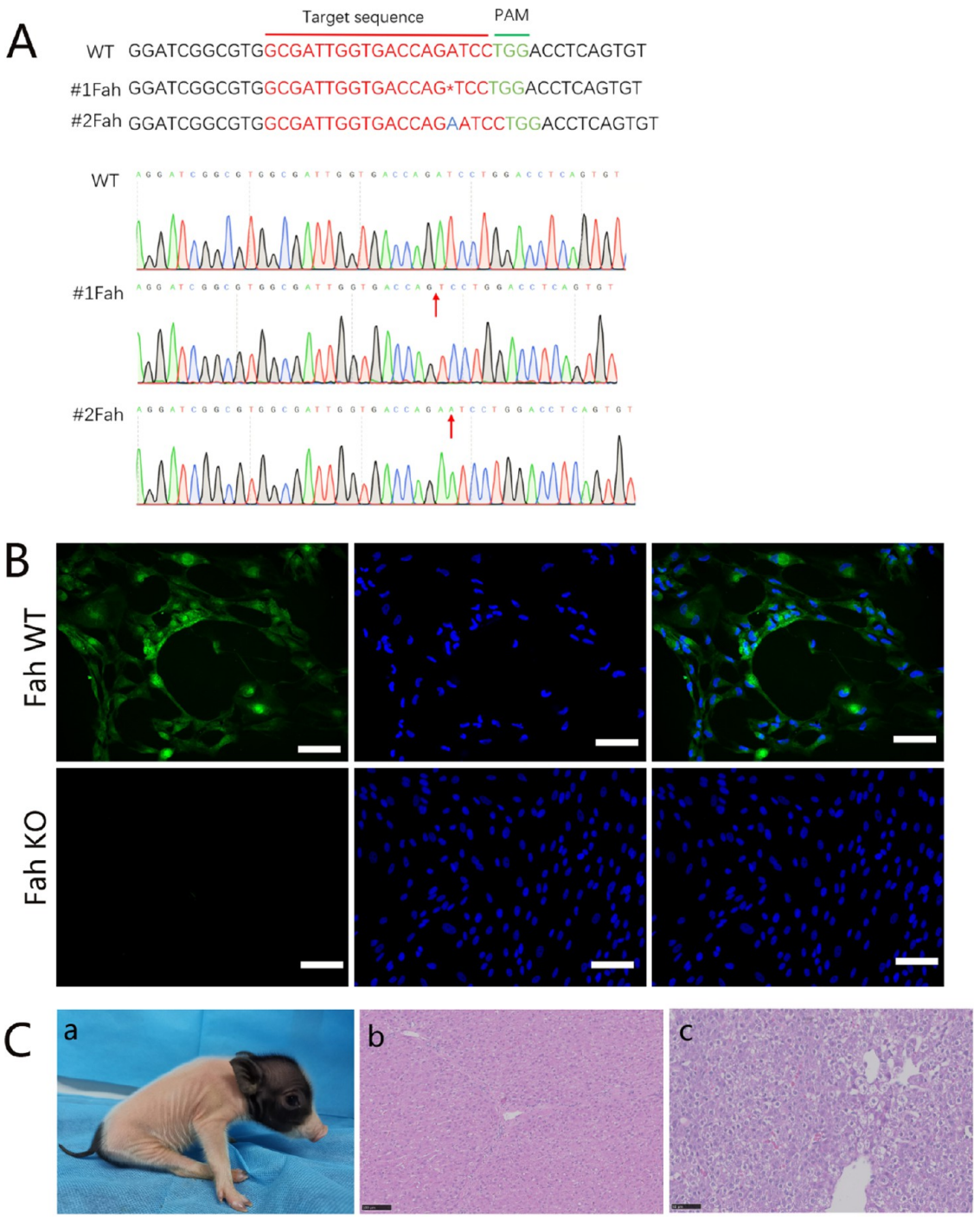

Figure 7. Generation of gene-edited pigs by SCNT using gene-edited monoclonal spheres from the microarray. (A) Sequencing analysis of gene-edited colonies generated by the CRISPR/Cas9 system. 1 bp deletion occurred in the #1*Fah* colony; 1 bp insertion occurred in the #2*Fah* colony. (B) Detection of protein expression in gene-edited cells by IF. Scale bar = 100 μm. (C) *Fah* gene-edited pig. (a) The *Fah*KO pig. (b, c) H&E showed the liver morphology of a wild-type pig and *Fah*KO pig. *Fah*KO: *Fah* knockout; WT: wild type; scale bar = 50 μm.

As shown in Figure 6C-g, after digestion, the monoclonal cell population obtained by the microarray method showed smooth edges and regular circles. After electric activation, the recombinant embryo showed a uniform cytoplasm and smooth cell membrane, and most of them met the requirements for transplantation to surrogate sows (Figure 6C-i). The percentage of successfully activated embryos in the clone ring group was significantly lower than that in the control group, and there were no significant differences between the microarray group and the control group (Figure 6D).

3.5. Generation of *Fah* Knockout Minipigs by SCNT.

The above results verified the high efficiency of using a microarray to obtain monoclonal cells and construct recombinant embryos. Then, three *Fah* colonies harvested from the microarray were randomly selected for analysis. The cell genotypes were analyzed by TA cloning and Sanger sequencing. The results demonstrated that two clones of *Fah* were biallelic mutations. The #1*Fah* colony showed a 1 bp deletion. A 1 bp insertion occurred in the #2*Fah* colony. These were typical indel

https://doi.org/10.1021/acsomega.2c01074
ACS Omega 2022, 7, 23156−23169

mutations caused by CRISPR/Cas9. One colony of *Fah* was wild type (Figure 7A).

The #1*Fah* colony was randomly selected as donor cells for SCNT. We also evaluated the protein expression of Fah in the cells by immunostaining (Figure 7B). Compared with WT cells, the knockout cells (KO) did not express Fah protein, indicating that *Fah* mutant cells were successfully obtained (Figure 7B).

To test whether the monoclonal cells obtained by this method could be used as nuclear transfer donors to deliver gene-edited pigs, 250 embryos were transplanted into a surrogate sow, the sow was successfully gestated, and two piglets were delivered. We then verified the genotype by gene sequencing and demonstrated that the two cloned piglets described above were all KO pigs. The H&E results showed edema and cytoplasmic ballooning degeneration in the livers of the pigs, which is consistent with the reported phenotype of *Fah*KO pigs (Figure 7C-b,c).

4. DISCUSSION

Genetically engineered pigs hold great promise in xenotransplantation, modeling human disease and regenerative medicine.[30] The advanced genome engineering tools of CRISPR/Cas9 accelerate the construction of a large animal model.[31] At present, the generation of genetically modified animals is mostly based on somatic cell nuclear transfer (SCNT) combined with CRISPR/Cas9 technology.[32] Therefore, the generation of gene-edited nuclear donors is crucial.[33] Currently, the nuclear donor cells used for SCNT are mainly porcine embryonic fibroblasts or porcine renal fibroblasts (PKFs).[34]

Nevertheless, these primary cells naturally proliferate slowly and are vulnerable. In addition, under normal circumstances, fibroblasts are not resistant to long-term culture and easily senesce. Continuous passage of more than 10 generations results in slow proliferation and morphological changes, and their karyotypes tend to become disordered, showing obvious characteristics of senescence.[9]

However, the transgenic operation of pig cells requires complicated procedures such as culture, transfection, resistance screening, and re-expansion culture, which usually takes approximately 20 days and passes for approximately five to seven generations.[35] The activity of somatic cells undergoing such an operation is significantly reduced, and their nuclear reprogramming ability is affected.[36] Furthermore, it will cause the surrogate sow to miscarry and the fetus to be deformed. Therefore, when preparing porcine-modified somatic cells, it is generally required to use high-activity cells with early generation and short cumulative culture times. Especially in the preparation of polygenic modified pigs, this issue needs to be considered.

In previous studies, the results showed that knocking out multiple copies of a gene or generating multigene-edited pigs requires continuous gene-editing experiments on cells, which results in cell apoptosis and poor conditions.[37] Researchers need to add many factors, such as p53 inhibitors, pifithrin α (PFTa), and basic fibroblast growth factor (bFGF), to maintain the cellular state and increase the average targeting efficiency.[38]

To overcome this problem, in this study, we innovatively reported that using kidney ECM pregel to pattern microarrays can quickly obtain gene-edited monoclonal cells in good condition. The success rate of constructing recombinant embryos using these monoclonal cells was significantly higher than that of the traditional cloning ring method.

Decellularized ECM derived from different organs provides an ideal tissue-specific microenvironment for cells, and the retained full biochemical complexity of the native tissue contributes to the regeneration of tissue or cells. Therefore, they have been utilized as coatings for cell culture.[39]

The frequently used decellularization method to prepare decellularized ECM from multiple organs is arterial perfusion with decellularization reagents.[40] In our previous studies, sequential perfusion with Triton X-100−SDS−Triton X-100 was shown to be effective in removing cellular components from porcine liver and kidney.[16] However, the unduly detergence of SDS can result in an excessive loss of ECM and crucial growth factors.[41] Recently, a novel anionic detergent, sodium lauryl ether sulfate (SLES), was reported to decellularize the rat heart and lung[21,24] and showed milder chemical properties and high biocompatibility capacity. In this study, we compared the properties of kidney ECM perfused with SDS and SLES and their biological activity.

The results of H&E staining and DAPI staining showed that no nuclear structure could be detected in the kidney after SDS and SLES perfusion, indicating that both SDS and SLES could effectively remove cell components in the tissue (Figure 2A,B).

The chemical structure analysis results of ECM showed that both the SDS- and SLES-treated ECMs contained carboxyl groups, hydroxyl groups, amino groups, and amide groups, which indicate the collagen proteoglycan components (Figure 3B). Further quantitative analysis showed that collagen and glycosaminoglycan components in the ECM were effectively retained, and these components in the SLES group were significantly higher than those in the SDS group (Figure 3C,D). Growth factors promote cell proliferation. The results showed that bFGF and VEGF, two common growth factors, were well preserved in ECMs, and the SLES group was significantly higher than the SDS group (Figure 3E,F). To more intuitively compare the differences between the two groups of ECMs, proteomic analysis showed that there were many different proteins in SDS-perfused ECM and SLES-perfused ECM, and the functions of these different proteins focused on cell differentiation and cell adhesion (Figure 3G,H).

Fibronectin, collagen I, collagen IV, and laminin are thought to be important ECM protein components for cell adhesion, proliferation, and differentiation. Our results also showed the proteins collagen I and IV and fibronectin laminin (Figure 4).

When using kidney ECM pregel as the coating reagent to culture PKFs, the results showed that kidney ECM pregel was more conducive to viability, adhesion, and proliferation than the uncoated and Matrigel coating groups (Figure 5). In addition, compared with Matrigel, a product of a tumorigenic cell line, there were no potential risks of ECM pregel coculture with nuclear donor cells. Moreover, PKFs showed significantly higher proliferation in the SLES coating group than in the SDS coating groups (Figure 5D,E).

In previous studies, cytokines were preserved in tissues or may be released into the microenvironment, further promoting cell and tissue growth.[42] Our results demonstrate that when ECM coating dishes were used, more growth factors were detected in cell supernatants, which explained why the cell proliferation rate in the ECM group was significantly higher than that in the untreated group and Matrigel group (Figure 5F,G). In addition, the SLSE group had a higher concentration of growth factor in the cell culture supernatant than the SDS group (Figure 5F,G). This result indicated that SLES detergent retains more biological components of tissues. The SLES-treated ECM is a more ideal coating substrate.

https://doi.org/10.1021/acsomega.2c01074
ACS Omega 2022, 7, 23156−23169

The status of gene-editing monoclonal cells used for nuclear donors directly affects the construction of recombinant embryos. The shorter the culture time of nuclear donor cells in vitro, the better. To shorten the operation generation of gene-edited cells as much as possible, we need to solve how the acquisition of enough monoclonal cells used to be the nuclear donor can be accelerated. Microarrays can limit cells to a specific adhesion space and allow them to cluster into spheres for a short time. To further optimize the chips and make them more suitable for the growth of primary cell monoclonal cells, we used SLES-treated ECM pregel to pattern the microarray to promote sphere formation of monoclonal cells and reduce the generations of cell reproduction.

In this study, we explored an ECM-based microarray to obtain high-quality gene-edited cell spheres. The gene-edited cells formed a three-dimensional dendritic (3D) structure after 96 h of culture in the 50 μm microarrays and then formed 3D cell microspheres. Because the contact surface between the microsphere and the culture bottom is narrow and the adhesion is not firm, when the cell spheres grow to a certain size, they will automatically fall off from the bottom by shaking or gently blowing with a pipette gun. The detached cell spheres were visible to the naked eye. These detached cell spheres were diluted, and spheres proliferating from a single cell were blown away in the pore plate and then cultured. In this way, gene-edited-positive cell clones can be obtained quickly by one or two subcultures (Figure 6B-e-h). By comparison, it takes approximately 1 month to obtain enough monoclonal cells by the traditional cloning ring method, and most cells undergo morphological changes (Figure 6B-a-d).

Compared with the monoclonal cells obtained by the traditional cloning ring method, the monoclonal cells obtained by the microarray method can provide higher-quality nuclear donors, and the success rate of recombinant embryos constructed by them is significantly higher than that obtained by the traditional method (Figure 6C,D). Furthermore, we also successfully used these monoclonal cells as nuclear donors to obtain gene-edited pigs.

5. CONCLUSIONS

In this study, a new descaling agent, SLES, was used for the first time to prepare a porcine kidney extracellular matrix pregel. Using the pregel as a substrate to pattern microarrays, we can promote cell proliferation and adhesion, maintain high cell viability, and enable single primary kidney fibroblasts to grow at a restricted site and spontaneously assemble into spherules within 4 days. Compared with the traditional monoclonal method, the harvesting time of monoclonal cells was reduced from 30−40 to 10 days, which greatly reduced the passage cycle of primary gene-edited cells in vitro and could provide high-quality nuclear donors for somatic cell nuclear transplantation in a better and faster way. Finally, monoclonal cells prepared by this method were used as nuclear donors to successfully produce *Fah* gene knockout pigs.

These monoclonal microarrays will have greater application potential in the construction of multigene knockout/knockin cells and could provide the conditions for fragile cells to proliferate after complex and long-term operation studies. Moreover, this single-cell patterning technology could also contribute to biological studies in vitro, such as the understanding of basic cell functions, cell behaviors, cell migration, and drug screening. In contrast to traditional population-based cell experiments, single-cell patterning is an effective technology for the in-depth study of fundamental cell characteristics and for fully understanding cell heterogeneity. Moreover, given that microarrays can promote cell clustering into spheres, microarrays can also be used to grow organoids. In the next step, we will expand the application of this microarray.

■ ASSOCIATED CONTENT

Supporting Information

The Supporting Information is available free of charge at https://pubs.acs.org/doi/10.1021/acsomega.2c01074.

Evaluation of cell spheres cultured in the micropattern array with different sizes (Figure S1) (PDF)

■ AUTHOR INFORMATION

Corresponding Authors

Ji Bao − *Institute of Clinical Pathology, Key Laboratory of Transplant Engineering and Immunology, West China Hospital, Sichuan University, Chengdu 610041, China;* orcid.org/0000-0001-8413-3270; Email: baoji@scu.edu.cn

Hong Bu − *Department of Pathology, West China Hospital, Sichuan University, Chengdu 610041, China; Institute of Clinical Pathology, Key Laboratory of Transplant Engineering and Immunology, West China Hospital, Sichuan University, Chengdu 610041, China*; Email: hongbu@scu.edu.cn

Authors

Mengyu Gao − *Department of Pathology, West China Hospital, Sichuan University, Chengdu 610041, China; Institute of Clinical Pathology, Key Laboratory of Transplant Engineering and Immunology, West China Hospital, Sichuan University, Chengdu 610041, China;* orcid.org/0000-0003-0269-9727

Xinglong Zhu − *Institute of Clinical Pathology, Key Laboratory of Transplant Engineering and Immunology, West China Hospital, Sichuan University, Chengdu 610041, China*

Wanliu Peng − *Institute of Clinical Pathology, Key Laboratory of Transplant Engineering and Immunology, West China Hospital, Sichuan University, Chengdu 610041, China*

Yuting He − *Institute of Clinical Pathology, Key Laboratory of Transplant Engineering and Immunology, West China Hospital, Sichuan University, Chengdu 610041, China*

Yi Li − *Precision Medicine Key Laboratory, West China Hospital, Sichuan University, Chengdu 610041, China*

Qiong Wu − *Institute of Clinical Pathology, Key Laboratory of Transplant Engineering and Immunology, West China Hospital, Sichuan University, Chengdu 610041, China*

Yanyan Zhou − *Institute of Clinical Pathology, Key Laboratory of Transplant Engineering and Immunology, West China Hospital, Sichuan University, Chengdu 610041, China*

Guangneng Liao − *Experimental Animal Center, West China Hospital, Sichuan University, Chengdu 610041, China*

Guang Yang − *Experimental Animal Center, West China Hospital, Sichuan University, Chengdu 610041, China*

Complete contact information is available at: https://pubs.acs.org/10.1021/acsomega.2c01074

Author Contributions

⊥M.G. and X.Z. contributed equally to this work.

Funding

This work was supported by the National Natural Scientific Foundations of China (81770618 and 82070640), the

Technology Innovation Project of Chengdu New Industrial Technology Research Institute (2018-CY02-00046-GX), and the Key R&D (Major Science and Technology Project) Project of Sichuan Science and Technology Department (2019YFS0138).

Notes

The authors declare no competing financial interest.

■ ACKNOWLEDGMENTS

The authors thank ShiSheng Wang and Yi Zhong (West China-Washington Mitochondria and Metabolism Research Center, West China Hospital, Sichuan University) for relative data acquisition and analysis and HuiFang Li (Core Facilities of West China Hospital, Sichuan University) for the flow cytometry analysis.

■ REFERENCES

(1) (a) Das, S.; Koyano-Nakagawa, N.; Gafni, O.; Maeng, G.; Singh, B. N.; Rasmussen, T.; Pan, X.; Choi, K. D.; Mickelson, D.; Gong, W.; et al. Generation of human endothelium in pig embryos deficient in ETV2. *Nat. Biotechnol.* **2020**, *38*, 297−302. (b) Hein, R.; Sake, H. J.; Pokoyski, C.; Hundrieser, J.; Brinkmann, A.; Baars, W.; Nowak-Imialek, M.; Lucas-Hahn, A.; Figueiredo, C.; Schuberth, H. J.; et al. Triple (GGTA1, CMAH, B2M) modified pigs expressing an SLA class I(low) phenotype-Effects on immune status and susceptibility to human immune responses. *Am. J. Transplant.* **2020**, *20*, 988−998. (C) Zhou, X.; Xin, J.; Fan, N.; Zou, Q.; Huang, J.; Ouyang, Z.; Zhao, Y.; Zhao, B.; Liu, Z.; Lai, S.; et al. Generation of CRISPR/Cas9-mediated gene-targeted pigs via somatic cell nuclear transfer. *Cell. Mol. Life Sci.* **2015**, *72*, 1175−1184.

(2) (a) Kubo, S.; Sun, M.; Miyahara, M.; Umeyama, K.; Urakami, K.; Yamamoto, T.; Jakobs, C.; Matsuda, I.; Endo, F. Hepatocyte injury in tyrosinemia type 1 is induced by fumarylacetoacetate and is inhibited by caspase inhibitors. *Proc. Natl. Acad. Sci. U.S.A.* **1998**, *95*, 9552−9557. (b) Orejuela, D.; Jorquera, R.; Bergeron, A.; Finegold, M. J.; Tanguay, R. M. Hepatic stress in hereditary tyrosinemia type 1 (HT1) activates the AKT survival pathway in the fah-/- knockout mice model. *J. Hepatol.* **2008**, *48*, 308−317.

(3) Azuma, H.; Paulk, N.; Ranade, A.; Dorrell, C.; Al-Dhalimy, M.; Ellis, E.; Strom, S.; Kay, M. A.; Finegold, M.; Grompe, M. Robust expansion of human hepatocytes in Fah-/-/Rag2-/-/Il2rg-/- mice. *Nat. Biotechnol.* **2007**, *25*, 903−910.

(4) (a) Cong, L.; Ran, F. A.; Cox, D.; Lin, S.; Barretto, R.; Habib, N.; Hsu, P. D.; Wu, X.; Jiang, W.; Marraffini, L. A.; Zhang, F. Multiplex genome engineering using CRISPR/Cas systems. *Science* **2013**, *339*, 819−823. (b) Wang, X.; Cao, C.; Huang, J.; Yao, J.; Hai, T.; Zheng, Q.; Wang, X.; Zhang, H.; Qin, G.; Cheng, J.; et al. One-step generation of triple gene-targeted pigs using CRISPR/Cas9 system. *Sci. Rep.* **2016**, *6*, No. 20620. (c) Yao, J.; Wang, Y.; Cao, C.; Song, R.; Bi, D.; Zhang, H.; Li, Y.; Qin, G.; Hou, N.; Zhang, N.; et al. CRISPR/Cas9-mediated correction of MITF homozygous point mutation in a Waardenburg syndrome 2A pig model. *Mol. Ther.–Nucleic Acids* **2021**, *24*, 986−999.

(5) (a) Fu, R.; Fang, M.; Xu, K.; Ren, J.; Zou, J.; Su, L.; Chen, X.; An, P.; Yu, D.; Ka, M.; et al. Generation of GGTA1-/-β2M-/-CIITA-/- Pigs Using CRISPR/Cas9 Technology to Alleviate Xenogeneic Immune Reactions. *Transplantation* **2020**, *104*, 1566−1573. (b) Gao, M.; Zhu, X.; Yang, G.; Bao, J.; Bu, H. CRISPR/Cas9-Mediated Gene Editing in Porcine Models for Medical Research. *DNA Cell Biol.* **2021**, *40*, 1462−1475.

(6) Yu, H.; Long, W.; Zhang, X.; Xu, K.; Guo, J.; Zhao, H.; Li, H.; Qing, Y.; Pan, W.; Jia, B.; et al. Generation of GHR-modified pigs as Laron syndrome models via a dual-sgRNAs/Cas9 system and somatic cell nuclear transfer. *J. Transl. Med.* **2018**, *16*, No. 41.

(7) Akhlaghpour, A.; Taei, A.; Ghadami, S. A.; Bahadori, Z.; Yakhkeshi, S.; Molamohammadi, S.; Kiani, T.; Samadian, A.; Ghezelayagh, Z.; Haghparast, N.; et al. Chicken Interspecies Chimerism Unveils Human Pluripotency. *Stem Cell Rep.* **2021**, *16*, 39−55.

(8) Zhu, X. X.; Zhong, Y. Z.; Ge, Y. W.; Lu, K. H.; Lu, S. S. CRISPR/Cas9-Mediated Generation of Guangxi Bama Minipigs Harboring Three Mutations in α-Synuclein Causing Parkinson's Disease. *Sci. Rep.* **2018**, *8*, No. 12420.

(9) (a) Zhu, X.; Wei, Y.; Zhan, Q.; Yan, A.; Feng, J.; Liu, L.; Tang, D. CRISPR/Cas9-Mediated Biallelic Knockout of IRX3 Reduces the Production and Survival of Somatic Cell-Cloned Bama Minipigs. *Animals* **2020**, *10*, No. 501. (b) Lee, J.; Lee, Y.; Lee, G. S.; Lee, S. T.; Lee, E. Comparative study of the developmental competence of cloned pig embryos derived from spermatogonial stem cells and fetal fibroblasts. *Reprod. Domest. Anim.* **2019**, *54*, 1258−1264.

(10) Kurome, M.; Geistlinger, L.; Kessler, B.; Zakhartchenko, V.; Klymiuk, N.; Wuensch, A.; Richter, A.; Baehr, A.; Kraehe, K.; Burkhardt, K.; et al. Factors influencing the efficiency of generating genetically engineered pigs by nuclear transfer: multi-factorial analysis of a large data set. *BMC Biotechnol.* **2013**, *13*, No. 43.

(11) Yang, R.; Lemaître, V.; Huang, C.; Haddadi, A.; McNaughton, R.; Espinosa, H. D. Monoclonal Cell Line Generation and CRISPR/Cas9 Manipulation via Single-Cell Electroporation. *Small* **2018**, *14*, No. e1702495.

(12) (a) Wang, Z.; Lang, B.; Qu, Y.; Li, L.; Song, Z.; Wang, Z. Single-cell patterning technology for biological applications. *Biomicrofluidics* **2019**, *13*, No. 061502. (b) Zhang, Y.; Gao, M.; Hu, M.; Zhang, B.; He, Y.; Li, S.; Bao, J.; Bu, H. Using the Patterned Microarray Culture to Obtain Gene-Editing Monoclonal Cells. *Transplant. Proc.* **2020**, *52*, 1906−1909. (c) Li, S.; Yang, K.; Chen, X.; Zhu, X.; Zhou, H.; Li, P.; Chen, Y.; Jiang, Y.; Li, T.; Qin, X.; et al. Simultaneous 2D and 3D cell culture array for multicellular geometry, drug discovery and tumor microenvironment reconstruction. *Biofabrication* **2021**, *13*, No. 045013.

(13) (a) Hadavi, E.; Leijten, J.; Brinkmann, J.; Jonkheijm, P.; Karperien, M. van Apeldoorn, A. Fibronectin and Collagen IV Microcontact Printing Improves Insulin Secretion by INS1E Cells. *Tissue Eng., Part C* **2018**, *24*, 628−636. (b) Miyamoto, D.; Hara, T.; Hyakutake, A.; Nakazawa, K. Changes in HepG2 spheroid behavior induced by differences in the gap distance between spheroids in a micropatterned culture system. *J. Biosci. Bioeng.* **2018**, *125*, 729−735.

(14) Choudhury, D.; Tun, H. W.; Wang, T.; Naing, M. W. Organ-Derived Decellularized Extracellular Matrix: A Game Changer for Bioink Manufacturing? *Trends Biotechnol.* **2018**, *36*, 787−805.

(15) Badylak, S. F.; Freytes, D. O.; Gilbert, T. W. Extracellular matrix as a biological scaffold material: Structure and function. *Acta Biomater.* **2009**, *5*, 1−13.

(16) Gao, M.; Wang, Y.; He, Y.; Li, Y.; Wu, Q.; Yang, G.; Zhou, Y.; Wu, D.; Bao, J.; Bu, H. Comparative evaluation of decellularized porcine liver matrices crosslinked with different chemical and natural crosslinking agents. *Xenotransplantation* **2019**, *26*, No. e12470.

(17) Li, Y.; Wu, Q.; Li, L.; Chen, F.; Bao, J.; Li, W. Decellularization of porcine whole lung to obtain a clinical-scale bioengineered scaffold. *J. Biomed. Mater. Res., Part A* **2021**, *109*, 1623−1632.

(18) O'Neill, J. D.; Freytes, D. O.; Anandappa, A. J.; Oliver, J. A.; Vunjak-Novakovic, G. V. The regulation of growth and metabolism of kidney stem cells with regional specificity using extracellular matrix derived from kidney. *Biomaterials* **2013**, *34*, 9830−9841.

(19) Saldin, L. T.; Cramer, M. C.; Velankar, S. S.; White, L. J.; Badylak, S. F. Extracellular matrix hydrogels from decellularized tissues: Structure and function. *Acta Biomater.* **2017**, *49*, 1−15.

(20) (a) Funamoto, S.; Nam, K.; Kimura, T.; Murakoshi, A.; Hashimoto, Y.; Niwaya, K.; Kitamura, S.; Fujisato, T.; Kishida, A. The use of high-hydrostatic pressure treatment to decellularize blood vessels. *Biomaterials* **2010**, *31*, 3590−3595. (b) Woods, T.; Gratzer, P. F. Effectiveness of three extraction techniques in the development of a decellularized bone-anterior cruciate ligament-bone graft. *Biomaterials* **2005**, *26*, 7339−7349.

(21) Kawasaki, T.; Kirita, Y.; Kami, D.; Kitani, T.; Ozaki, C.; Itakura, Y.; Toyoda, M.; Gojo, S. Novel detergent for whole organ tissue engineering. *J. Biomed. Mater. Res., Part A* **2015**, *103*, 3364−3373.

https://doi.org/10.1021/acsomega.2c01074
ACS Omega 2022, 7, 23156−23169

(22) Naeem, E. M.; Sajad, D.; Talaei-Khozani, T.; Khajeh, S.; Azarpira, N.; Alaei, S.; Tanideh, N.; Reza, T. M.; Razban, V. Decellularized liver transplant could be recellularized in rat partial hepatectomy model. *J. Biomed. Mater. Res., Part A* **2019**, *107*, 2576−2588.
(23) Keshvari, M. A.; Afshar, A.; Daneshi, S.; Khoradmehr, A.; Baghban, M.; Muhaddesi, M.; Behrouzi, P.; Miri, M. R.; Azari, H.; Nabipour, I.; et al. Decellularization of kidney tissue: comparison of sodium lauryl ether sulfate and sodium dodecyl sulfate for allotransplantation in rat. *Cell Tissue Res.* **2021**, *386*, 365−378.
(24) Ma, J.; Ju, Z.; Yu, J.; Qiao, Y.; Hou, C.; Wang, C.; Hei, F. Decellularized Rat Lung Scaffolds Using Sodium Lauryl Ether Sulfate for Tissue Engineering. *ASAIO J.* **2018**, *64*, 406−414.
(25) (a) Wagner, D. E.; Bonenfant, N. R.; Sokocevic, D.; DeSarno, M. J.; Borg, Z. D.; Parsons, C. S.; Brooks, E. M.; Platz, J. J.; Khalpey, Z. I.; Hoganson, D. M.; et al. Three-dimensional scaffolds of acellular human and porcine lungs for high throughput studies of lung disease and regeneration. *Biomaterials* **2014**, *35*, 2664−2679. (b) Gilpin, S. E.; Guyette, J. P.; Gonzalez, G.; Ren, X.; Asara, J. M.; Mathisen, D. J.; Vacanti, J. P.; Ott, H. C. Perfusion decellularization of human and porcine lungs: bringing the matrix to clinical scale. *J. Heart Lung Transplant.* **2014**, *33*, 298−308.
(26) Wu, Q.; Bao, J.; Zhou, Y. J.; Wang, Y. J.; Du, Z. G.; Shi, Y. J.; Li, L.; Bu, H. Optimizing perfusion-decellularization methods of porcine livers for clinical-scale whole-organ bioengineering. *Biomed. Res. Int.* **2015**, *2015*, No. 785474.
(27) Zhou, C.; Zhou, L.; Liu, J.; Xu, L.; Xu, Z.; Chen, Z.; Ge, Y.; Zhao, F.; Wu, R.; Wang, X.; et al. Kidney extracellular matrix hydrogel enhances therapeutic potential of adipose-derived mesenchymal stem cells for renal ischemia reperfusion injury. *Acta Biomater.* **2020**, *115*, 250−263.
(28) Kang, Y.; Kim, S.; Bishop, J.; Khademhosseini, A.; Yang, Y. The osteogenic differentiation of human bone marrow MSCs on HUVEC-derived ECM and β-TCP scaffold. *Biomaterials* **2012**, *33*, 6998−7007.
(29) Gao, M.; Zhang, B.; He, Y.; Yang, Q.; Deng, L.; Zhu, Y.; Lai, E.; Wang, M.; Wang, L.; Yang, G.; Liao, G.; Bao, J.; Bao, J.; Bu, H. Efficient Generation of an Fah/Rag2 Dual-Gene Knockout Porcine Cell Line Using CRISPR/Cas9 and Adenovirus. *DNA Cell Biol.* **2019**, *38*, 314−321.
(30) (a) Zou, X.; Ouyang, H.; Yu, T.; Chen, X.; Pang, D.; Tang, X.; Chen, C. Preparation of a new type 2 diabetic miniature pig model via the CRISPR/Cas9 system. *Cell Death Dis.* **2019**, *10*, 823. (b) Wu, J.; Platero-Luengo, A.; Sakurai, M.; Sugawara, A.; Gil, M. A.; Yamauchi, T.; Suzuki, K.; Bogliotti, Y. S.; Cuello, C.; Morales Valencia, M.; et al. Interspecies Chimerism with Mammalian Pluripotent Stem Cells. *Cell* **2017**, *168*, 473−486.e415.
(31) (a) Sykes, M.; Sachs, D. H. Transplanting organs from pigs to humans. *Sci. Immunol.* **2019**, *4*, No. eaau6298. (b) Zuo, E.; Cai, Y. J.; Li, K.; Wei, Y.; Wang, B. A.; Sun, Y.; Liu, Z.; Liu, J.; Hu, X.; Wei, W.; et al. One-step generation of complete gene knockout mice and monkeys by CRISPR/Cas9-mediated gene editing with multiple sgRNAs. *Cell Res.* **2017**, *27*, 933−945.
(32) Yan, S.; Tu, Z.; Liu, Z.; Fan, N.; Yang, H.; Yang, S.; Yang, W.; Zhao, Y.; Ouyang, Z.; Lai, C.; et al. A Huntingtin Knockin Pig Model Recapitulates Features of Selective Neurodegeneration in Huntington's Disease. *Cell* **2018**, *173*, 989−1002.e1013.
(33) Samiec, M.; Skrzyszowska, M. Intrinsic and extrinsic molecular determinants or modulators for epigenetic remodeling and reprogramming of somatic cell-derived genome in mammalian nuclear-transferred oocytes and resultant embryos. *Pol. J. Vet. Sci.* **2018**, *21*, 217−227.
(34) Zhu, X. X.; Zhan, Q. M.; Wei, Y. Y.; Yan, A. F.; Feng, J.; Liu, L.; Lu, S. S.; Tang, D. S. CRISPR/Cas9-mediated MSTN disruption accelerates the growth of Chinese Bama pigs. *Reprod. Domest. Anim.* **2020**, *55*, 1314−1327.
(35) Wang, K.; Jin, Q.; Ruan, D.; Yang, Y.; Liu, Q.; Wu, H.; Zhou, Z.; Ouyang, Z.; Liu, Z.; Zhao, Y.; et al. Cre-dependent Cas9-expressing pigs enable efficient in vivo genome editing. *Genome Res.* **2017**, *27*, 2061−2071.
(36) Jin, L.; Guo, Q.; Zhang, G. L.; Xing, X. X.; Xuan, M. F.; Luo, Q. R.; Luo, Z. B.; Wang, J. X.; Yin, X. J.; Kang, J. D. The Histone Deacetylase Inhibitor, CI994, Improves Nuclear Reprogramming and In Vitro Developmental Potential of Cloned Pig Embryos. *Cell. Reprogram.* **2018**, *20*, 205−213.
(37) Yang, L.; Güell, M.; Niu, D.; George, H.; Lesha, E.; Grishin, D.; Aach, J.; Shrock, E.; Xu, W.; Poci, J.; et al. Genome-wide inactivation of porcine endogenous retroviruses (PERVs). *Science* **2015**, *350*, 1101−1104.
(38) (a) Niu, D.; Wei, H. J.; Lin, L.; George, H.; Wang, T.; Lee, I. H.; Zhao, H. Y.; Wang, Y.; Kan, Y.; Shrock, E.; et al. Inactivation of porcine endogenous retrovirus in pigs using CRISPR-Cas9. *Science* **2017**, *357*, 1303−1307. (b) Yue, Y.; Xu, W.; Kan, Y.; Zhao, H. Y.; Zhou, Y.; Song, X.; Wu, J.; Xiong, J.; Goswami, D.; Yang, M.; et al. Extensive germline genome engineering in pigs. *Nat. Biomed. Eng.* **2021**, *5*, 134−143.
(39) (a) Zhang, Y.; He, Y.; Bharadwaj, S.; Hammam, N.; Carnagey, K.; Myers, R.; Atala, A.; Van Dyke, M. Tissue-specific extracellular matrix coatings for the promotion of cell proliferation and maintenance of cell phenotype. *Biomaterials* **2009**, *30*, 4021−4028. (b) DeQuach, J. A.; Mezzano, V.; Miglani, A.; Lange, S.; Keller, G. M.; Sheikh, F.; Christman, K. L. Simple and high yielding method for preparing tissue specific extracellular matrix coatings for cell culture. *PLoS One* **2010**, *5*, No. e13039.
(40) (a) Baptista, P. M.; Siddiqui, M. M.; Lozier, G.; Rodriguez, S. R.; Atala, A.; Soker, S. The use of whole organ decellularization for the generation of a vascularized liver organoid. *Hepatology* **2011**, *53*, 604−617. (b) Wang, Y.; Bao, J.; Wu, Q.; Zhou, Y.; Li, Y.; Wu, X.; Shi, Y.; Li, L.; Bu, H. Method for perfusion decellularization of porcine whole liver and kidney for use as a scaffold for clinical-scale bioengineering engrafts. *Xenotransplantation* **2015**, *22*, 48−61.
(41) Momtahan, N.; Panahi, T.; Poornejad, N.; Stewart, M. G.; Vance, B. R.; Struk, J. A.; Castleton, A. A.; Roeder, B. L.; Sukavaneshvar, S.; Cook, A. D. Using Hemolysis as a Novel Method for Assessment of Cytotoxicity and Blood Compatibility of Decellularized Heart Tissues. *ASAIO J.* **2016**, *62*, 340−348.
(42) (a) Hoganson, D. M.; Owens, G. E.; O'Doherty, E. M.; Bowley, C. M.; Goldman, S. M.; Harilal, D. O.; Neville, C. M.; Kronengold, R. T.; Vacanti, J. P. Preserved extracellular matrix components and retained biological activity in decellularized porcine mesothelium. *Biomaterials* **2010**, *31*, 6934−6940. (b) Chun, S. Y.; Lim, G. J.; Kwon, T. G.; Kwak, E. K.; Kim, B. W.; Atala, A.; Yoo, J. J. Identification and characterization of bioactive factors in bladder submucosa matrix. *Biomaterials* **2007**, *28*, 4251−4256. (c) Ali, M.; Pr, A. K.; Yoo, J. J.; Zahran, F.; Atala, A.; Lee, S. J. A Photo-Crosslinkable Kidney ECM-Derived Bioink Accelerates Renal Tissue Formation. *Adv. Healthcare Mater.* **2019**, *8*, No. e1800992.

https://doi.org/10.1021/acsomega.2c01074
ACS Omega 2022, 7, 23156−23169